7. ANKARA INTERNATIONAL AEROSPACE CONFERENCE
11-13 September 2013 - METU, Ankara TURKEY

AIAC-2013-109

LARGE EDDY SIMULATION OF COMPRESSIBILE FLOW AROUND NACA 0012 AIRFOIL AT STALL CONDITION

Farshad Rezaei[1], Ehsan Roohi[2], Mahmoud Pasandideh-Fard[3]

High Performance Computing (HPC) Laboratory, Department of Mechanical Engineering, Ferdowsi University of Mashhad, P.O.BOX: 91775-1111, Mashhad, Iran

ABSTRACT

In this paper, the effect of compressibility on stall behavior of NACA0012 airfoil at a Reynolds number of $3.98\text{x}10^6$ is studied using the OpenFOAM package. Large Eddy Simulation (LES) turbulence model is used to simulate flow at high angle of attack in near-stall or stall condition. Different grid sizes have been examined and the suitable mesh whose C_L and C_D are close to the experimental data had been presented. It is observed that at an angle of attack of 18° and Mach number of 0.2, the compressibility does not have a major effects and incompressible simulation gives more accurate results, whereas at a flow field with Mach number of 0.25 the compressible simulation is necessary. The influence of vortexes formation, movement and separation is investigated on the lift, drag and wall pressure coefficients. It is shown that these vortexes cause the pressure distribution to have a fluctuating behavior on the upper surface of the airfoil. This behavior causes the airfoil to be unstable and has serious implications in term of achievable performance at stall condition.

INTRODUCTION

In the last decades, computational fluid dynamics (CFD) has become the preferred method for predicting aerodynamic performance during aircraft design. In particular, aerodynamic analysis at stall with massive separation is especially important when evaluating an aircraft's ability to take off and land. Dynamic stall is an unsteady instability typically associated with flow separation. The stall vortex is formed around its leading edge and travels along the airfoil surface as it grows, and finally separates from the airfoil surface near the trailing edge. Instability of the stall grows with flow separation and eventually prevents the wing's ability to create lift. Stall flow simulation by using Reynolds-averaged Navier-Strokes (RANS) methods has many difficulties due to unsteady vortical flows. RANS methods intend to model the large scale eddies using a universal model. Large scale turbulence is affected by the flow geometry and boundary conditions and a universal model does not exist. On the other hand, Large Eddy Simulation (LES) is promising to overcome the disadvantages of the RANS model. In LES, the governing equations are spatially filtered on the scale of the numerical grid. The large energy containing scales are directly simulated, and the small scale eddies, which are generally more homogeneous and universal, are modeled. The large eddies are strongly affected by the flow field geometry boundaries. Therefore, the direct computation of the large eddies by LES is more accurate than the modeling of the large eddies using RANS.
Ladson [7] experimentally investigated the aerodynamic characteristics of the NACA 0012 airfoil in different Reynolds and Mach number and his results are used to validate the current simulation. The high value of the Reynolds number ($Re \geq 10^6$) and the complexity of the different turbulent boundary layers (including transitional phenomena and separations) still

[1] M.Sc. Student, Ferdowsi University of Mashhad, farshad_r585@yahoo.com
[2] Assistant Professor, Ferdowsi University of Mashhad, e.roohi@um.ac.ir
[3] Associate Professor, Ferdowsi University of Mashhad, fard_m@um.ac.ir

render the simulation of flow over the high lift airfoils unaffordable. Therefore recent works of several researchers have been dedicated to the simulation of two dimensional isolated profiles, which represents a first step toward the real configuration [5,6,18]. The stability of the simulation often requires the use of some numerical dissipation, which deteriorates the efficiency of the subgrid scale (SGS) modeling. Consequently, LES of flow around an isolated airfoil still demands an effort to improve the numerical techniques and evaluate the solution sensitiveness to numerical parameters, such as the SGS modeling and the grid resolution. Mary and Sagaut [9] used LES of a turbulent flow past an airfoil near stall at a chord Reynolds number of 2.1×10^6. They used a local mesh-refinement technique and a discretization of the convective fluxes in a block-structured finite volume code to reduce the total number of grid points and the numerical dissipation acting on the small scales, respectively. They had investigated the influence of subgrid scale modeling and showed that the computed mean and fluctuating velocity profiles compare favorably with the experimental measurements. Soshi et al. [15] investigated the capability of large-eddy simulation (LES) with wall-modeling in predicting transitional and separated flow over an airfoil near stall condition at high Reynolds number. They showed that by incorporating the non-equilibrium effects and transition treatment in the wall model, the wall-modeled LES well predicts the mean and turbulence statistics in the region of laminar separation, turbulent transition, turbulent reattachment, and initial-mid developments of attached turbulent boundary layer. Also, comparisons between the non-equilibrium and equilibrium wall-models highlighted the importance of including the non-equilibrium effects in the model. Moreau et al. [10] performed LES of the trailing edge flow and noise of a NACA0012 airfoil near stall condition. Dahlstrom [1] concerned the efforts of conducting a Large Eddy Simulation around an airfoil in his work. He had found that the treatment of the laminar region has a major effect on the turbulent boundary layer further downstream. Martinat et al. [8] provided a study of the NACA0012 dynamic stall at Reynolds number 10^5 and 10^6 by means of two- and three-dimensional numerical simulations. The turbulence effect on the dynamic stall is also studied by statistical modeling. He concluded that standard URANS turbulence modeling has shown a quite dissipative character that attenuates the instabilities and the vortex structures related to the dynamic stall. Wang et al. [17] presented a 2D computational investigating on the dynamic stall phenomenon associated with unsteady flow around the NACA0012 airfoil at low Reynolds number ($Re_c \approx 10^5$). He concluded that the CFD prediction captures well the vortex-shedding predominated flow structure which is experimentally obtained. The results quantitatively agree well whit the experimental data, except when the blade is at a very high angle of attack. Im et al. [4] performed DES (Detached Eddy Simulation) and DDES (Delayed Detached Eddy Simulation) of NACA0012 airfoil near stall condition. They showed that DDES and DES predicted the drag coefficient accurately, while URANS (unsteady Reynolds-averaged Navier-Stokes) over predicted the drag by 33.6%. Different researchers employed OpenFOAM for aerodynamic proposes. For example, Richez et al. [12] investigated the course of events leading to stall just before its occurrence and LES of the flow around an airfoil profile at high angle of attack (AOA) had been achieved. Analysis of his results underlines the strong effect of the laminar separation bubble (LSB) structure on the whole downstream flow and, in particular, on the length of turbulent separation at the trailing edge. He also employed a zonal RANS/LES hybrid method and showed there is a good agreement with the LES in the separated flow. According to our best knowledge, there is not any detailed investigation considering compressibility effects on separated flow field around NACA0012.

Accurate numerical simulation of flow field over external geometries needs considering different points such as employing suitable grid size (especially in the boundary layer), applying accurate discretization model (specifically near stall condition), and for LES simulation, consideration of suitable SGS models. This paper investigates the capability of LES with one equation SGS model in simulation of separated flow over a NACA0012 airfoil at stall condition at high Reynolds number using the open source CFD package of OpenFOAM. Within the framework of OpenFOAM, *pisoFoam* solver have used for incompressible LES and *rhoPimpleFoam* solver for compressible LES. The PISO (Pressure

Implicit with Splitting of Operators) is an efficient method to solve the Navier-Stokes equations in unsteady incompressible problems. This algorithm uses iterative procedures for solving equations for velocity and pressure, PISO being used for transient problems.
The numerical simulation reported in the present work has been conducted using OpenFOAM 2.1.0 code. OpenFoam has attracted much attention recently because it is a sustainable open source code designed for a wide range of CFD applications. It is a C++ toolbox based on object oriented programming [16]. OpenFOAM is released under the GPL [3,11] and it consists of enormous groups of libraries for different mathematical, numerical and physical models. Linking the mathematical/numerical tools with the physical models in a main C++ function produces different solvers and utilities. OpenFOAM allows the users freely choose among a wide range of numerical discretization and interpolation schemes.

LES MODEL

Large eddy simulation (LES) is based on computing the large, energy-containing structures that are resolved on the computational grid, whereas the smaller, more isotropic, sub-grid structures are modeled [13]. In contrast to RANS approaches, which are based on solving for an ensemble average of the flow properties, LES naturally and consistently allows for medium to small scale, transient flow structures. Starting from the incompressible Navier-Stokes (NS) equations, the governing flow equations consists of the balance equations of mass and momentum,

$$\begin{aligned} &\partial_t(\rho v) + \nabla.(\rho v \times v) = -\nabla p + \nabla.s, \\ &\partial_t \rho + \nabla.(\rho v) = 0 \end{aligned} \tag{1}$$

where v is the velocity, p is the pressure, $s = 2\mu D$ is the viscous stress tensor, where the rate-of-strain tensor is expressed as

$$D = \frac{1}{2}\left(\nabla v + \nabla v^T\right) \tag{2}$$

where μ is the viscosity. The LES equations are theoretically derived, following e.g. Sagaut [14] from Eq. (1). In ordinary LES, all variables, i.e., f, are split into grid scale (GS) and subgrid scale (SGS) components, $f = \overline{f} + f'$, where $\overline{f} = G * f$ is the GS component, $G = G(X, \Delta)$ is the filter function, and $\Delta = \Delta(\mathbf{x})$ is the filter width. The LES equations result from convolving the NS with G, viz.,

$$\begin{aligned} &\partial_t(\rho\overline{v}) + \nabla.(\rho\overline{v} \times \overline{v}) = -\nabla\overline{p} + \nabla.(\overline{s} - B), \\ &\partial_t \rho + \nabla.(\rho\overline{v}) = 0 \end{aligned} \tag{3}$$

where over-bar denotes filtered quantity. Equation (3) introduces one new term when compared to the unfiltered Eq. (1): the unresolved transport term B, which is the sub grid stress tensor. Following Fureby [2], B can be exactly decomposed as

$$B = \rho.\left(\overline{\overline{v} \times \overline{v}} - \overline{\overline{v}} \times \overline{\overline{v}} + \tilde{B}\right) \tag{4}$$

where now only $\tilde{B}$ needs to be modeled. The most common subgrid modeling approaches utilizes an eddy or subgrid viscosity, v_{SGS}, similar to the turbulent viscosity approach in RANS, where v_{SGS} can be computed in a wide variety of methods. In eddy-viscosity models often,

$$B = \tfrac{2}{3}\overline{\rho} k l - 2\mu_k \breve{D}_D \tag{5}$$

where k is the SGS kinetic energy, μ_k the SGS eddy viscosity, and D_D the SGS eddy diffusivity. In the current study, subgrid scale terms are modeled using “one equation eddy viscosity" model. In order to obtain *k*,one-equation eddy-viscosity model (OEEVM) uses the following equation:

$$\sigma_t(\bar{\rho}k)+\nabla.(\bar{\rho}k\breve{V})=-B.(\mu\nabla k)+\bar{\rho}\varepsilon \tag{6}$$

Where

$$\varepsilon=\frac{C_\varepsilon k^{3/2}}{\Delta} \qquad \mu_k=C_k\bar{\rho}\Delta\sqrt{k} \tag{7}$$

Numerical Algorithm

The finite-volume method was employed to solve the governing equations in the computational domain. The numerical schemes for terms, such as derivatives in equations, is listed in table 1.

Table 1: Numerical schemes

Variable	Incompressible	Compressible
Pressure gradient	Fourth order	Gauss linear
Velocity gradient	Gauss linear	Gauss linear
Convection divergence	Gauss gamma	Gauss filtered linear2 V
First time derivative	backward	backward

The fourth order scheme in pressure gradient uses least squares technique. The Gauss keyword specifies the standard finite volume discretization of Gaussian integration which is second order and requires the interpolation of values from cell centers to face centers. Therefore, the Gauss entry must be followed by the choice of interpolation scheme such as linear, upwind, NVD schemes and TVD schemes. It would be extremely unusual to select anything other than general interpolation schemes and in most cases the linear scheme is an effective choice. Linear interpolation uses central differencing [11].
In divergence schemes, the Gauss scheme is the only choice of discretization and requires a selection of the interpolation scheme for the dependent field, i.e. *U*. The interpolation scheme for incompressible simulation is selected from NVD schemes and that is gamma scheme. For compressible simulation filtered linear 2v interpolation scheme is used. Filtered linear 2 is from upwinded convection schemes and it is Linear with filtering for high-frequency ringing. There are improved versions of some of the limited schemes for vector fields in which the limiter is formulated to take into account the direction of the field. These schemes are selected by adding V to the name of the general scheme like filtered linear 2V [11].
The time derivative term of the transient time scheme implemented in our model used the backward scheme, which is the second order and implicit scheme available in OpenFOAM for solving ordinary differential equations [11].
The setting of the initial and boundary conditions for velocity and pressure are established as shown in Table 2.

Table 2: Initial and boundary conditions

Variable	Initial	Inlet	Outlet	Wall
Pressure (P)	10^5 (pa)	ZG	Incompressible: FV	ZG
			Compressible: WT	
Velocity (U)	85 (m/s)	FV	ZG	FV

ZG: zero gradient FV: fixed value WT: wave transmissive

RESULTS AND DISCUSSION

Grid independency

The computational domain and applied boundary condition is schematically shown in figure 1. The grid employed in the present study is shown in figure 2.The flow field around NACA 0012 airfoil at velocities of 68 m/s (Ma=0.2) and 85 m/s (Ma=0.25) and a chord Reynolds number of 3.98×10^6 for simulating stall condition at AOA=18° is considered. The chord length of the airfoil for flow with Ma=0.2 is 0.85 *m* and for Ma=0.25 is 0.68 *m* and the employed turbulence model is LES using one equation eddy for subgrid model. Different meshes had been produced and the accuracy of numerical solution is investigated. Meshes information are given in table 3.

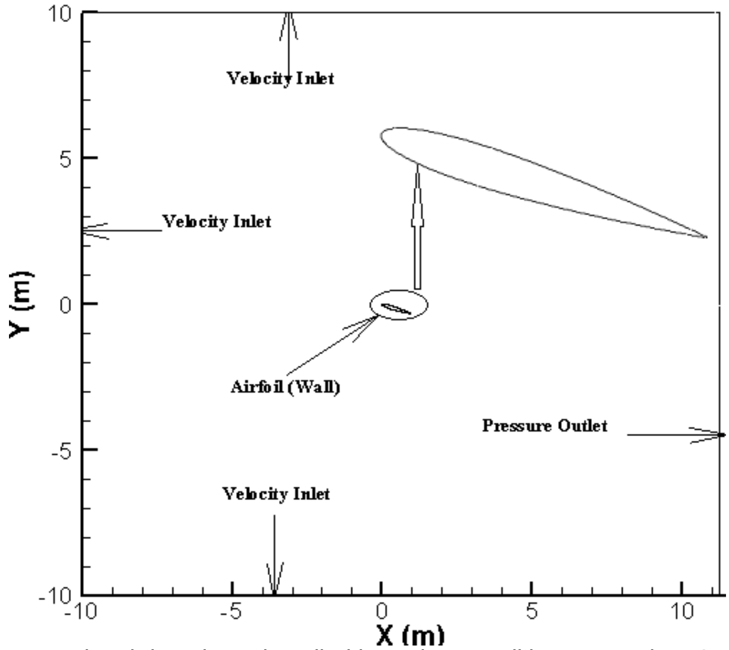

Figure 1: Computational domain and applied boundary conditions around NACA 0012 airfoil

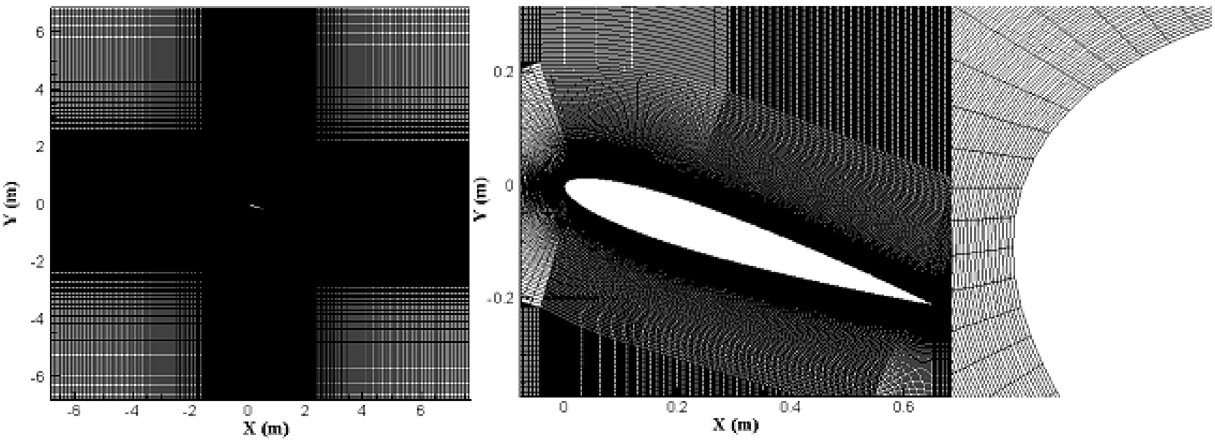

Figure 2: Computational grid with close-up views near leading edge

Table 3: Meshes properties

Mesh Name	Thickness of first B.L cell (mm)	Ratio of B.L in *y* direction	Number of points around the airfoil
Grid 1	0.6	1.06	370
Grid 2	0.3	1.03	610
Grid 3	0.1	1.003	810
Grid 4	0.1	1.0003	970

Lift and Drag coefficients for all four meshes are shown in figure 3. Ladson's experimental results [7] are used for comparing the current numerical simulation and experimental data. Figure 3 shows that the best result is given by grid 4 which is close to Ladson's experimental data.

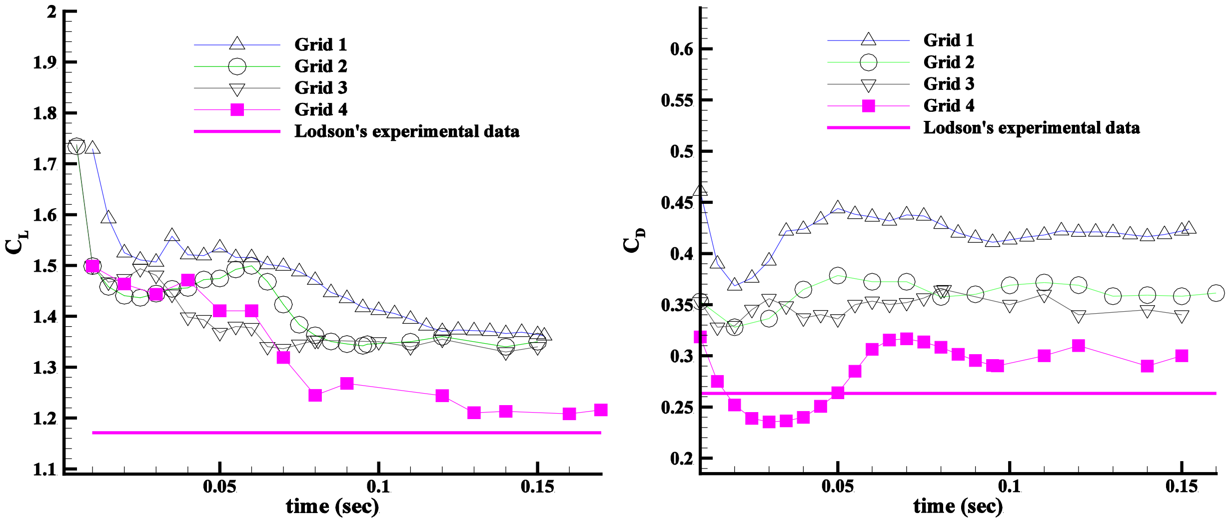

Figure 3: C_L & C_D Variations vs. time from the current LES numerical work for different grids compared with the numerical data of Ref. [7]

Effect of compressibility

The flow field around the airfoil at velocity of 68 m/s (Ma=0.2), AOA=18° and a chord Reynolds number of 3.98x10^{6} is considered. The simulation has been performed assuming both incompressible and compressible flow and lift and drag coefficients are showed in figure 4. It is observed that for mach 0.2, incompressible simulation gives better results than compressible simulation. In this case (Ma=0.2 and Re=3.98x10^{6}), experimental data [7] for C_L is 1.073 and C_D is 0.2753 and figure 4 shows that incompressible simulation is close to these data. This issue shows that at Ma=0.2 the effect of compressibility is weak even at 18 degree angle of attack.

Figure 5 shows C_L and C_D for both compressible and incompressible flow field around the airfoil at velocity of 85 *m/s* (Ma=0.25), AOA=18° and chord Reynolds number of 3.98x10^{6}. Experimental data for this case is 1.171 for C_L and 0.2632 for C_D, which is reported by Ladson [7]. It is observed that at this condition, compressible simulation gives more accurate C_L and C_D than incompressible simulation. In the flow field with Ma=0.25 at stall condition there are some regions with Ma≥0.3 and compressible flow will occur, so for accurate simulation it is important to consider these compressibility effects.

Figures 4 and 5 show that at initial times lift and drag coefficients in the incompressible simulation are so close to experimental data, because, on the one hand, at the mentioned times most parts of flow is incompressible and regions with compressibility effect have not been appeared yet. On the other hand, vortexes have not been formed. After that, vortexes are formed gradually and affect the wall pressure coefficient. Also, some parts with compressible characteristic flow are appeared. It is clear that by increase in time, lift and drag coefficients have a fluctuation behavior. So the average of lift and drag coefficients are computed.

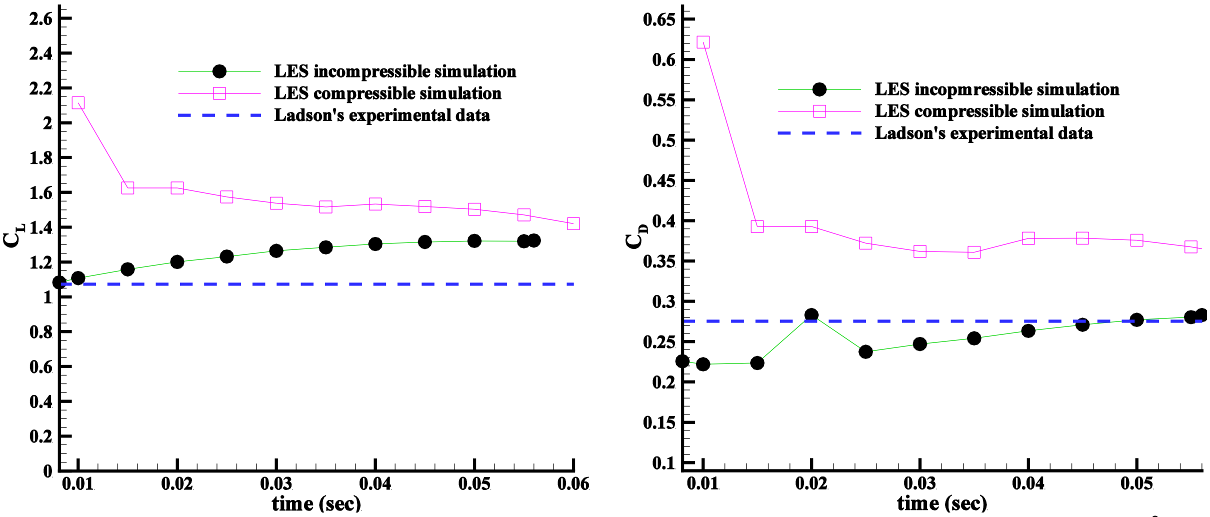

Figure 4: C_L & C_D Variations vs. time from the current LES numerical work at Ma=0.2 and Re=3.98x10^6 compared with the numerical data of Ref. [7]

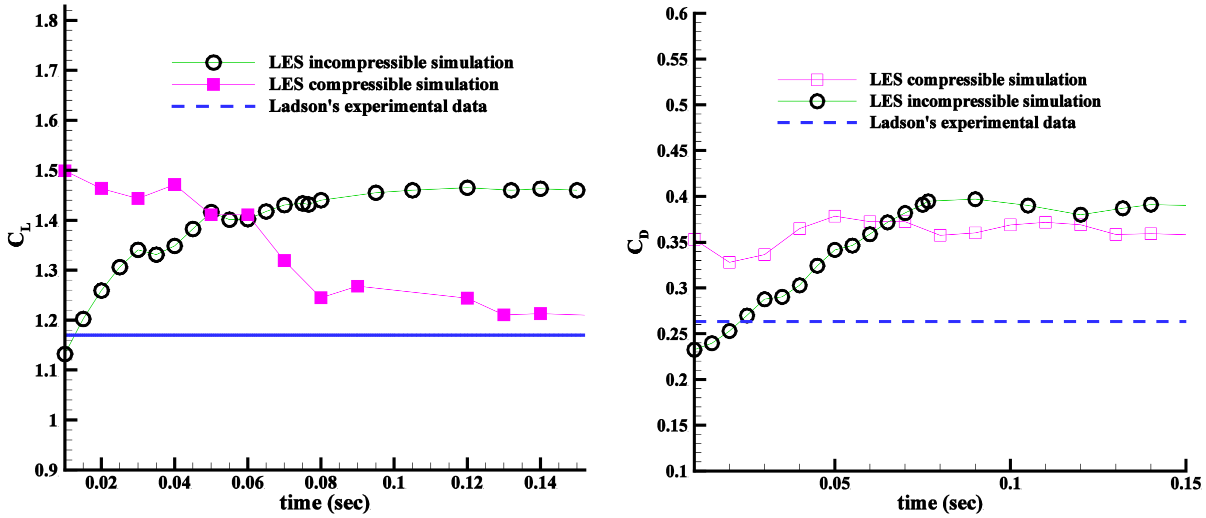

Figure 5: C_L & C_D Variations vs. time from the current LES numerical work at Ma=0.25 and Re=3.98x10^6 compared with the numerical data of Ref. [7]

For Ma=0.25 case, we compare compressible and incompressible vortex behaviors. Figure 6 shows velocity contours at different times and their appropriate wall pressure coefficients. Top frames show whole airfoil while middle and bottom row depict zoomed view of the leading edge and trailing edge of the airfoil. It is observed that as the time goes forward, some vortexes appear and move in line on the upper surface of the airfoil, and separate along the way of upper surface. The process of formation and separation of vortexes are repeated. Formation and separation of vortexes are unsteady, but by increasing the time, there are always some vortexes on the upper surface of the airfoil.
Pressure distribution shows that vortexes cause to have a fluctuation behavior in the pressure distribution on the upper surface of airfoil. So, the pressure center and other aerodynamic forces center are moved towards the leading edge and fluctuated in the first half of the chord. This subject causes the airfoil to be unstable and has serious implications in terms of achievable performance, which needs to be predicted accurately in the airfoil design cycle.

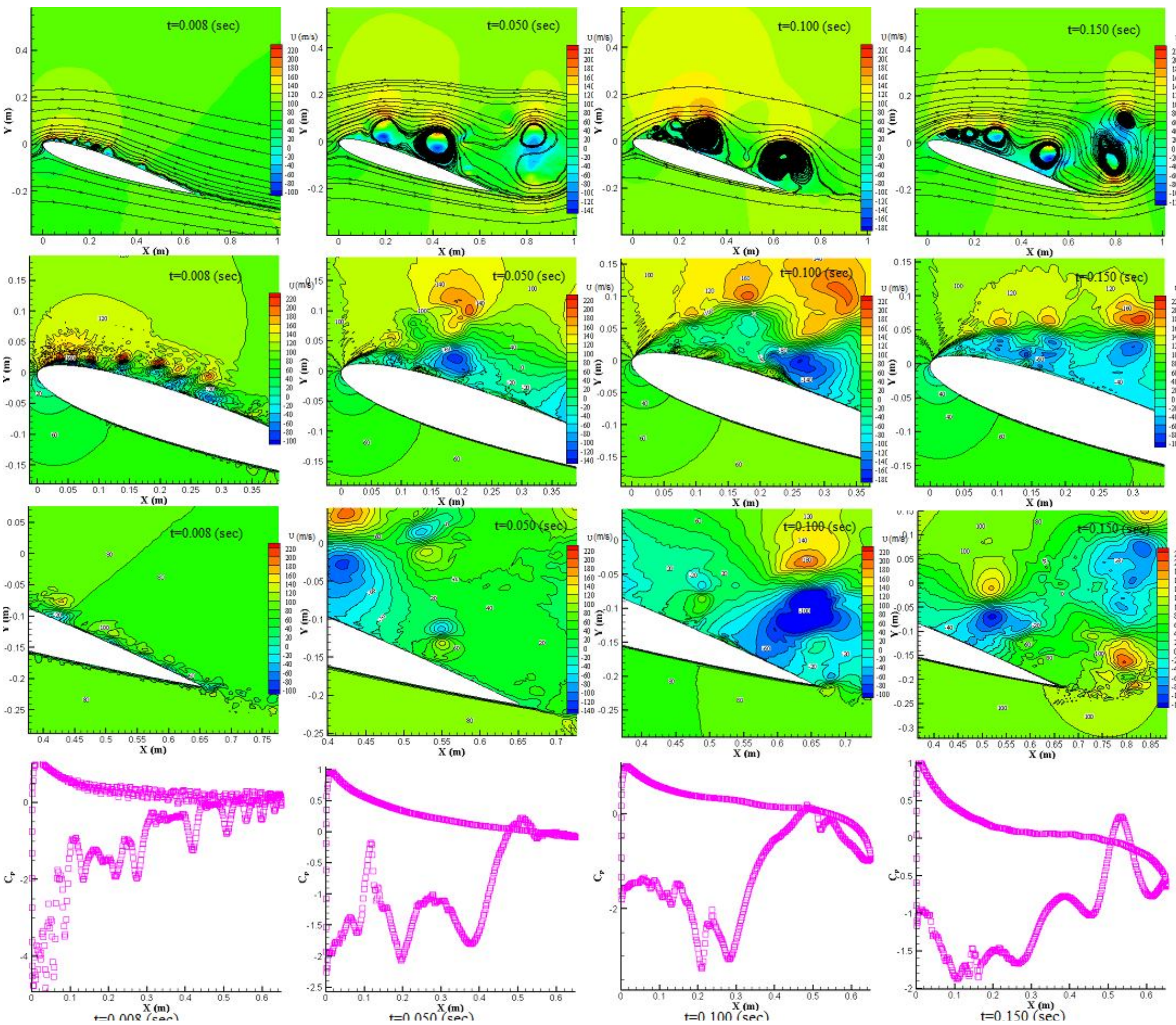

Figure 6: Formation, movement and separation of vortexes on the upper surface of the airfoil and their effects on the wall pressure coefficients at Ma=0.25 and Re=3.98x10^6, compressible solution

Figure 7 shows incompressible solution of the same test case and at the same time step as Fig. 6. Incompressible solution predicts less number of vortices over the airfoil, additionally, the vortices are smaller. These results in prediction of higher amount of lift in comparison with the experimental data, see Fig. 5.

Relevant density field of the compressible test case is shown in Fig. 8. The variations of density is shown in this figure confirms the need for compressible solution.

Conclusions

In this work, the effects of compressibility of flow field over NACA0012 airfoil at stall condition at high Reynolds number is investigated by using LES. It is shown that at Mach number of 0.2, incompressible simulation provides accurate solution for the flow field than compressible simulation, but once Mach number increases to 0.25, compressible simulation is necessary. Vortexes are observed on the upper surface of airfoil. The vortices move along the surface and separate as they arrive near the trailing edge of the airfoil. The influence of vortexes is to have fluctuation behavior in the wall pressure coefficient. It is realized that these vortexes cause aerodynamic forces center to move towards the leading edge.

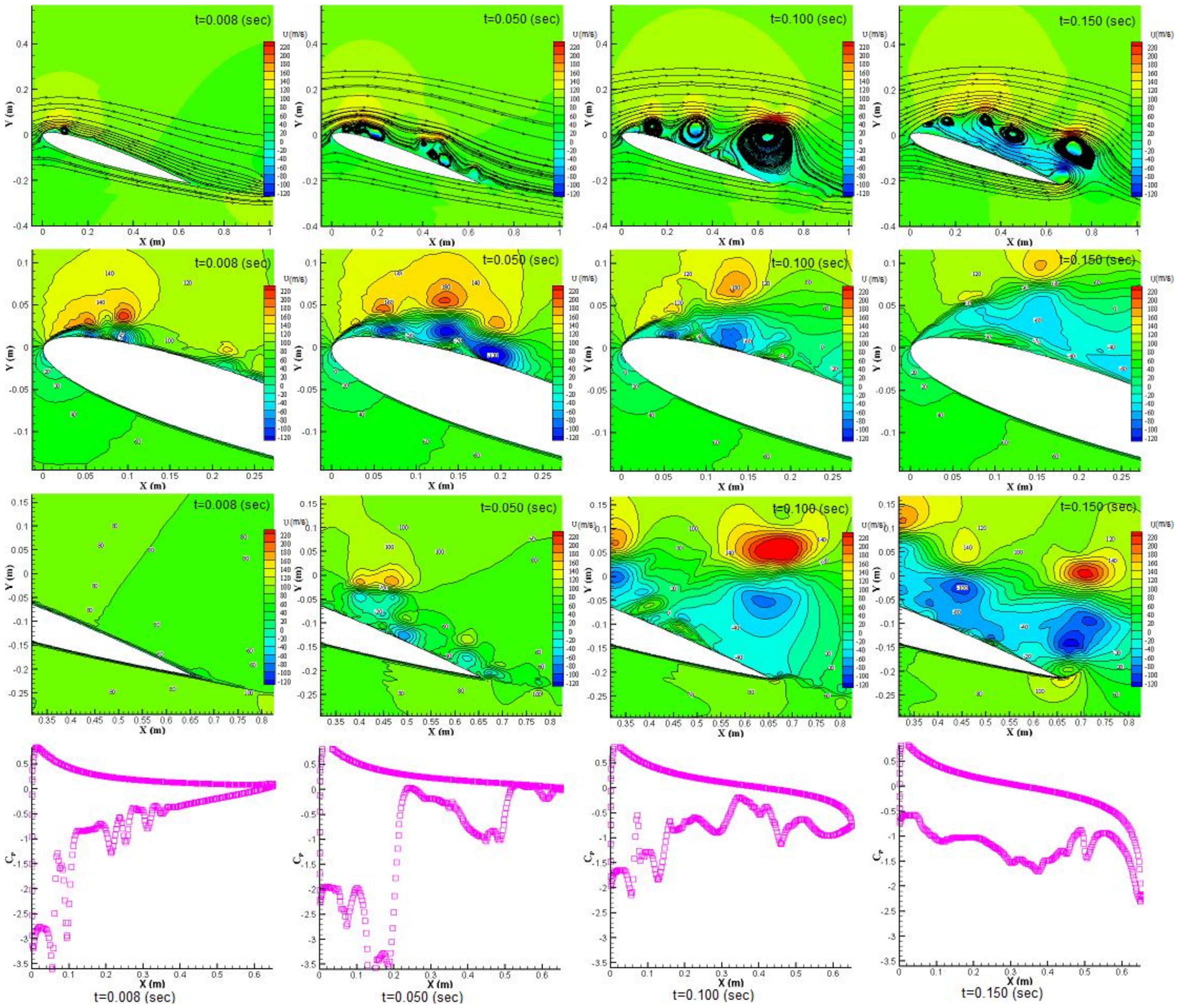

Figure 7: Formation, movement and separation of vortexes on the upper surface of the airfoil and their effects on the wall pressure coefficients at Ma=0.25 and Re=3.98x10^6, incompressible solution

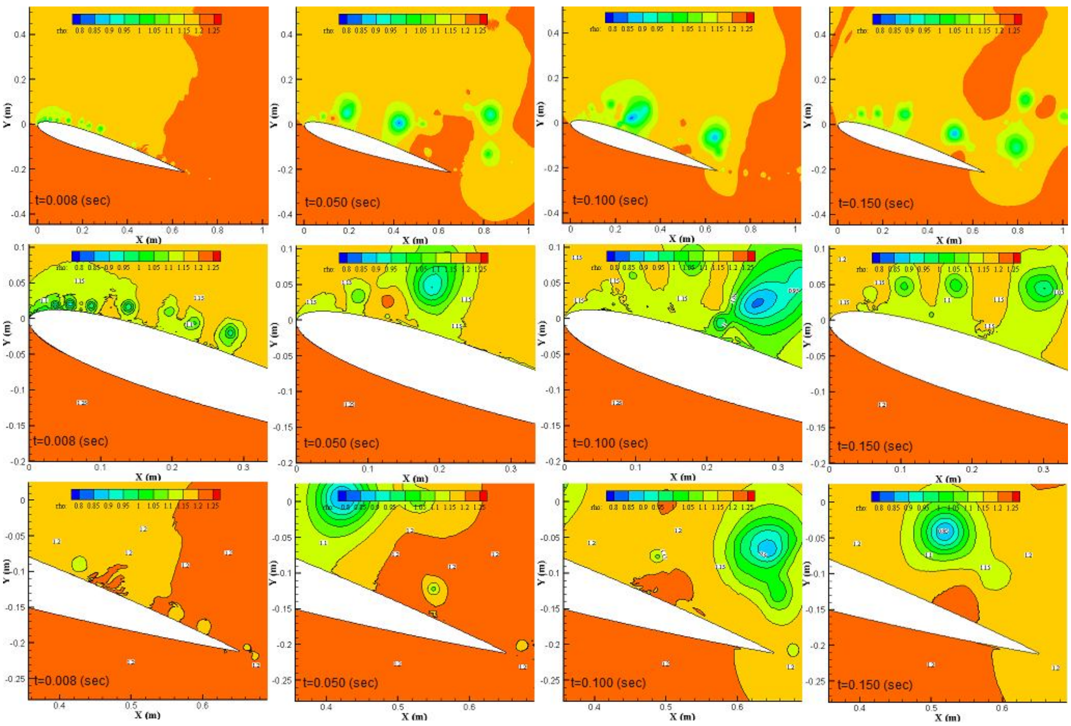

Figure 8: Density contour relevant to Fig. 6

References

[1] Dahlstrom, S., (2003) *Large Eddy Simulation of the Flow Around a High-Lift Airfoil* , Master of Science Thesis, Chalmers University of Technology, 2003.

[2] Fureby, C., and Grinstein, F., (2002) *Large Eddy Simulation of High-Reynolds Number Free and Wall-Bounded Flows*, journal of Computational Physics,Vol.181, pp. 68–97, 2002.

[3] http://www.openfoam.com.

[4] IM, H.S. and Zha, G.C., (2011) *Delayed Detached Eddy Simulation of a Stall Flow over NACA0012 Airfoil Using High Order Schemes*, AIAA-1297 2011.

[5] Jansen, K. , (1994) *Unstaructured-Grid Large-Eddy Simulation of Flow over an Airfoil*, Annual Research Brief, Center for Turbulence Research, Nasa Ames Research Center/Stanford Univ., Stanford, CA, pp. 161-175, 1994.

[6] Kaltenbach, H. J., and Choi,H., (1995) *Large-Eddy Simulation of Flow over an Airfoil on Structured Meshes*, Annual Research Brief, Center for Turbulence Research, Nasa Ames Research Center/Stanford Univ., Stanford, CA, pp. 51-61, 1995.

[7] Ladson, C.H, (1988) *Effects of Independent Variation of Mach and Reynolds Numbers on the Low-Speed Aerodynamics Characteristics of the NACA0012 Airfoil Section*, NASA TM 4074 report, 1988.

[8] Martinat, G., Braza, M., Hoarau, Y. and Harran, G., (2008) *Turbulence modeling of the flow past a pitching NACA0012 airfoil at 10^5 and 10^6 Reynolds number*, Journal of Fluids and Structures 24, PP 1294-1303, 2008.

[9] Mary, I., Sagaut, P., (2002) *Large Eddy Simulation of Flow Around an Airfoil Near Stall*, AIAA Journal, Vol. 40, No. 6, June 2002.

[10] Moreau, S., Christophe, J. and Roger, M., (2008) *Les of the trailing-edge flow and noise of a NACA0012 airfoil near stall*, Proceeding of the summer program, Center for Turbulence Research,2008.

[11] OpenFOAM, OpenFoam user guide. (2011).

[12] Richez, F., Mary, I., Gleize, V. and Basdevant, C., (2008) *Near stall simulation of the flow around an airfoil using zonal RANS/LES coupling method*, Computers & Fluids 37, PP 857-866 2008.

[13] Roohi, E., Zahiri, A. P., Passandideh-Fard, M., (2012) *Numerical Simulation of Cavitation around a Two-Dimensional Hydrofoil Using VOF Method and LES Turbulence Model*, Applied Mathematical Modeling, In press, 2013, DOI: 10.1016/j.apm, 2012.

[14] Sagaut T, P., (2006) *Large Eddy Simulation for Incompressible Flows*, Springer, New York, 3rd edition, 2006.

[15] Soshi, K., Kengo.A., (2012) *Wall-modeled large-eddy simulation of high Reynolds number flow around an airfoil near stall condition*, Computers & Fluids, november 2012

[16] Tabor, H.G., Jask,H.,Furbey,C., (1998) *A tensorial approach to computational continuum mechanics using object-oriented techniques*, Compute. Phys. (6), 1998.

[17] Wang. S., Ingham. D.B., Ma. L., Pourkashian. M. and Tao. Z., (2010) *Numerical investigations on dynamic stall of low Reynolds number flow around oscillating airfoils*, Computers & Fluids 39, PP 1529-1541, 2010.

[18] Weber, C., Ducros, F., (2000) *Large Eddy and Reynolds-Averaged Navier-stokes Simulation of Turbulent Flow over an Airfoil*, International of Journal of Computational Fluid Dynamics, Vol 13, pp. 327-355, 2000.